Scientific Reports

https://doi.org/10.1038/s41598-026-47203-4

Article in Press

# The earliest known ceramic beads as adornment from Nanzhuangtou site in North China 10,000 years ago

Received: 19 October 2025

Accepted: 30 March 2026

Published online: 03 April 2026

Cite this article as: Chen J., Zhao J., Li J. *et al.* The earliest known ceramic beads as adornment from Nanzhuangtou site in North China 10,000 years ago. *Sci Rep* (2026). https://doi.org/10.1038/s41598-026-47203-4

**Jianxiang Chen, Jingfang Zhao, Jun Li, Wenrui Zhang, Kai Wang, Xueyan Ren, Wanli Zhao & Wen Gao**

# The earliest known ceramic beads as adornment from Nanzhuangtou site in North China 10,000 years ago

Jianxiang Chen[1], Jingfang Zhao[1,*], Jun Li[2], Wenrui Zhang[3], Kai Wang[1], Xueyan Ren[3], Wanli Zhao[1] & Wen Gao[1]

**Abstract**: The innovation of artificial materials marks a pivotal advancement in human technology. However, direct evidence of their earliest symbolic application remains scarce. In this paper, two tubular ceramic beads were studied, approximately 10,000-year-old, from the Nanzhuangtou site in North China. These beads represent among the earliest known ornaments made from a fully synthetic material, with their age constrained to approximately 10,000 cal BP through stratigraphic association with directly dated materials. A multi-analytical approach was employed, incorporating X-ray fluorescence, high-resolution micro-computed tomography, scanning electron and optical microscopy, and Fourier transform infrared spectroscopy. This approach was used to demonstrate that the beads were fabricated from locally sourced clay. They were formed around a plant stem to create a hollow structure, and were fired at low temperatures (around 500–600□). Their morphological attributes strongly suggest that they were used as personal adornments. This discovery provides crucial empirical evidence that nascent pottery technology was used for symbolic expression during the critical Palaeolithic-Neolithic transition, thus extending the known chronology of the decorative use of synthetic materials by millennia.

**Keywords**: Ceramic beads, Nanzhuangtou site, Palaeolithic-Neolithic transition, Personal adornment



Personal ornaments are fundamental to people's understanding of the evolution of human symbolism, social identity, and cognitive complexity. Globally, the earliest personal ornaments, dating to approximately 300,000–100,000 years ago, were made from perforated natural materials such as marine shells, animal teeth, and bone[1]. This tradition of utilizing natural substances continued throughout the Palaeolithic in Europe, Asia, and Africa, with stone, ivory, and mollusc shells serving as the primary media[12]. In China, although the emergence of prehistoric ornaments was relatively late[3]3, sites such as Xiaogushan[4], Shuidonggou[5] and Zhoukoudian Upper Cave[6] have yielded an abundance of perforated ornaments from the Middle-Late Palaeolithic. This is consistent with the global pattern of selecting materials based on hardness and workability[7].

The transition from the Palaeolithic to the Neolithic era was marked by a significant technological shift: the invention of pottery. While the initial focus of pottery technology was probably utilitarian, it had the potential of creating new forms of material culture, including ornaments. During the early and middle Neolithic periods

[1] College of Applied Arts and Science, Beijing Union University, Beijing 100191, China
[2] School of Archaeology and Museology, Shanxi University, Taiyuan 030006, China
[3] Hebei Provincial Institute of Cultural Relics and Archaeology, Shijiazhuang 050031, China
* Corresponding author. email: jingfang@buu.edu.cn

in China, various pottery ornaments, such as rings and pendants, were produced[8]. In addition to China, the production of faience beads in the pre-3rd millennium BCE Egypt represents another significant early chapter in the history of synthetic materials[9]. Despite this broader context, detailed scientific studies specifically addressing the manufacturing techniques of early ceramic ornaments, particularly those with intentional hollow structures from the Palaeolithic-Neolithic transition, remain strikingly limited.

This research gap is significant, as the Palaeolithic-Neolithic transition was a pivotal moment in human technological and social development. Physical evidence of the use of of emerging pottery technology for the production of personal adornment during this critical period is extremely rare. This leaves key questions regarding the raw material choices, forming techniques, firing conditions, and functional attributes of the earliest ceramic ornaments unanswered. A comprehensive understanding of this innovation requires a multi-analytical scientific approach.

The tubular ceramic beads studied in this paper were excavated from gully G1 at the Nanzhuangtou site in the Xushui District of Hebei Province, China (Fig. 1a). The Nanzhuangtou site[910] is a crucial benchmark for the Palaeolithic-Neolithic transition in northern China, with radiocarbon dates placing its earliest layers at around 11,000 years BP. The site has yielded rich assemblages, including early pottery sherds, bone and antler tools, and stone artefacts, providing a well-defined context for early technological innovations. Within this context, the two beads (designated TZ1 and TZ2, Fig. 1b) offer a unique opportunity to investigate the initial steps of artificial adornments creation. This paper employs a multi-analytical scientific approach to elucidate the material composition, manufacturing technology, and functional use of these significant artifacts.

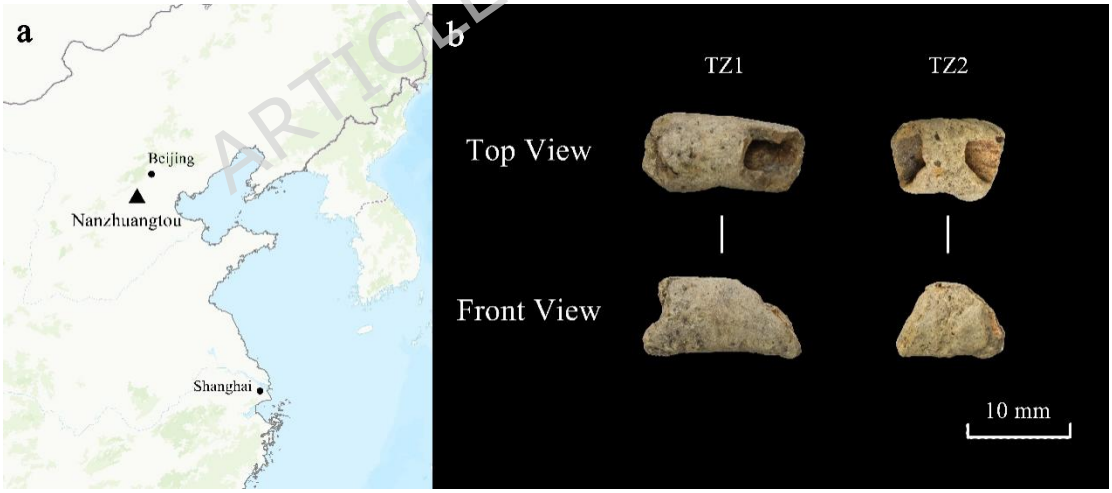


**Figure 1.** Site location and excavated beads. (a) Geographical location of the Nanzhuangtou site in North China. (b) Photographs of the two tubular ceramic beads (TZ1 and TZ2) analysed in this study, unearthed from gully G1.

## Materials

The two tubular ceramic beads (designated TZ1 and TZ2) analyzed in this study were discovered during the sorting of sieved materials from gully G1 at the Nanzhuangtou site. The natural gully G1 is an archaeological feature that was excavated in 1997. It was sealed beneath layer ③ of the site (Fig. 2), which has a radiocarbon date of 9535

BP[9], with a calibrated result of 11175 cal BP (Tab. 1 and Fig. 3a). Radiocarbon dating of a wood sample from gully G1 yielded a calibrated date of approximately 10,000 years BP (Tab. 1 and Fig. 3b), which further corroborates the chronology. This chronological context firmly places the beads within the Palaeolithic-Neolithic transition period in northern China.

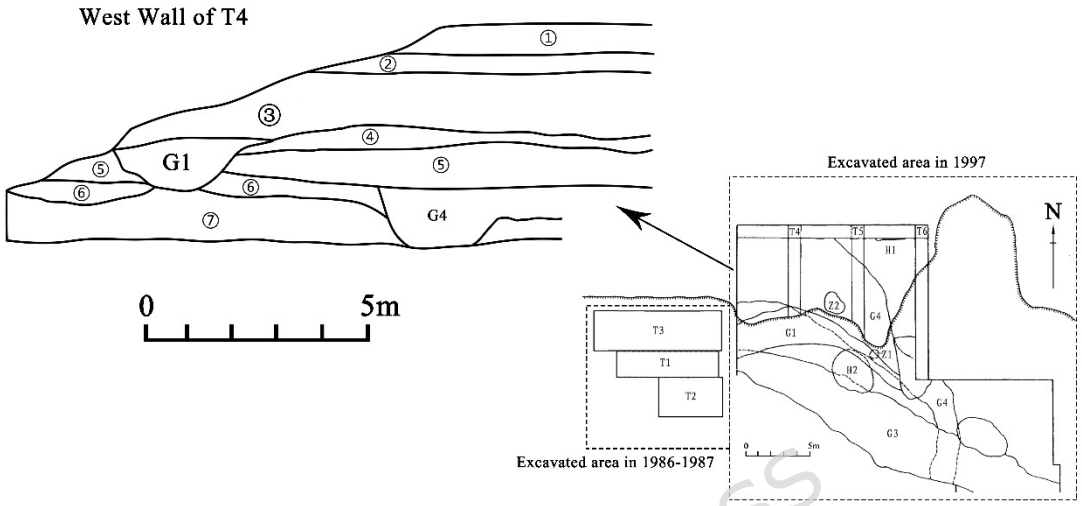


**Figure 2.** The section drawing of the west wall of Trench T4 reveals that Feature G1 was sealed beneath Layer ③ and cut through the underlying Layers ①, ⑤, ⑥, and ⑦.

**Table 1.** Radiocarbon dating results from layer ③ and G1 of the Nanzhuangtou site

| Laboratory | Sample ID | Lab Number | Sample | Determination Result | | |
|---|---|---|---|---|---|---|
| | | | | Uncalibrated age (BP) | Tree-ring calibrated age | |
| | | | | | 1σ | 2σ |
| Peking University AMS $^{14}$C Lab | XNT3③ | BK87083 | Bottom layer silt in the middle of T3 north wall | 9535±100 | 11080(30.9%)10921cal BP<br>10891(37.4%)10693cal BP | 11175(95.4%)10581cal BP |
| | G1 | BA250999 | G1 sieved material-wood | 8590±35 | 9593(5.2%)9581cal BP<br>9556(63.0%)10693cal BP | 9663(3.7%)9641cal BP<br>9631(84.4%)9521cal BP<br>9515(7.3%)9488cal BP |

Note: The uncalibrated dates in Column 1 are cited from the Excavation Report of 1987, while Column 2 shows the G1 dating results supplemented by the research team in 2025; Calibration was performed using the IntCal20 atmospheric curve (Reimer et al. 2020) and the OxCal v4.4.4 program (Bronk Ramsey, 2021).

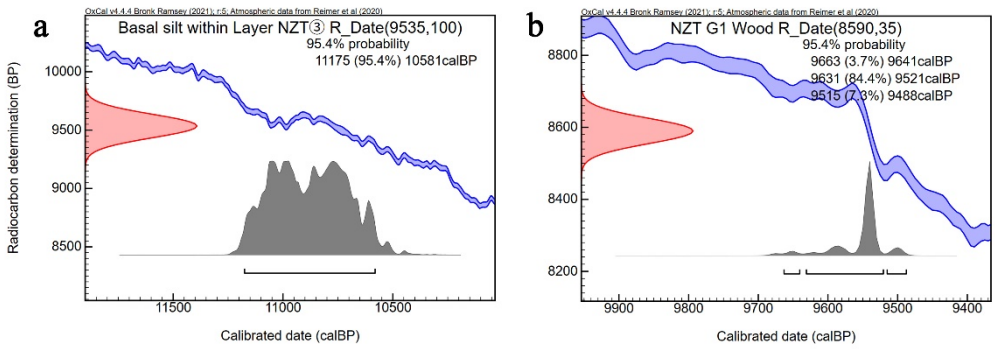

**Figure 3.** Radiocarbon dating results from (a) layers ③ and (b) G1 at the Nanzhuangtou site. The uncalibrated date of layer ③ was obtained from the excavation report[10], and the G1 dating results were supplemented by the research team in 2025. Two radiocarbon dating results were obtained from the Peking University AMS $^{14}C$ Laboratory. Calibration was performed via the IntCal20 atmospheric curve (Reimer *et al*. 2020) and the OxCal v4.4.4 program (Bronk Ramsey, 2021).

The two beads share comparable material properties and morphologies, suggesting that they belong to the same type of ceramic product or may even be parts of the same object. They are both hollow and made from fine, clay gray-brown pottery. They have partially greenish outer surfaces and reddish-brown inner surfaces. The tube walls are thin, approximately 1–2 mm thick. One end is shorter than the other, resulting in a trapezoidal profile. TZ1 measures approximately 9 mm (shorter end), 16 mm (longer end), and 7 mm in diameter. The corresponding dimensions for TZ2 are 3 mm, 11 mm, and 7 mm.

## Results and Discussion

**Local resource utilization: insights from chemical composition.** The results of energy-dispersive X-ray fluorescence spectroscopy (Appendix A, Tab. S1) indicate that the chemical compositions of TZ1 and TZ2 are highly consistent. Both exhibit elevated Fe□O□ content (Fig. 4), with higher concentrations on the inner surfaces compared to the outer surfaces, while the opposite trend is observed for SiO□. This compositional consistency, coupled with the systematic differences between the inner and outer surfaces, suggests that the two beads were manufactured using the same clay and technique. A comparison with data from early pottery sherds unearthed from Layer 5 at the Nanzhuangtou site (Appendix A, Tab. S2) reveals that the beads' chemical composition aligns with the "high-silica, low-alumina" characteristics of the site's early buff-brown pottery. Except for Fe, the other elemental compositions are relatively similar. Principal component analysis (Fig. 5) shows that the chemical composition of the beads' outer surfaces is closer to that of buff-brown pottery and local soil. In contrast, the inner (hollow) surfaces show greater divergence, which is attributable to their elevated iron content. According to the excavation report[11], the raw material for early buff-brown pottery was pure silty clay (alluvial soil) from beneath the cultural layer, which matches the characteristics of the bead specimens. This suggests that the raw clay for the two beads was sourced locally.

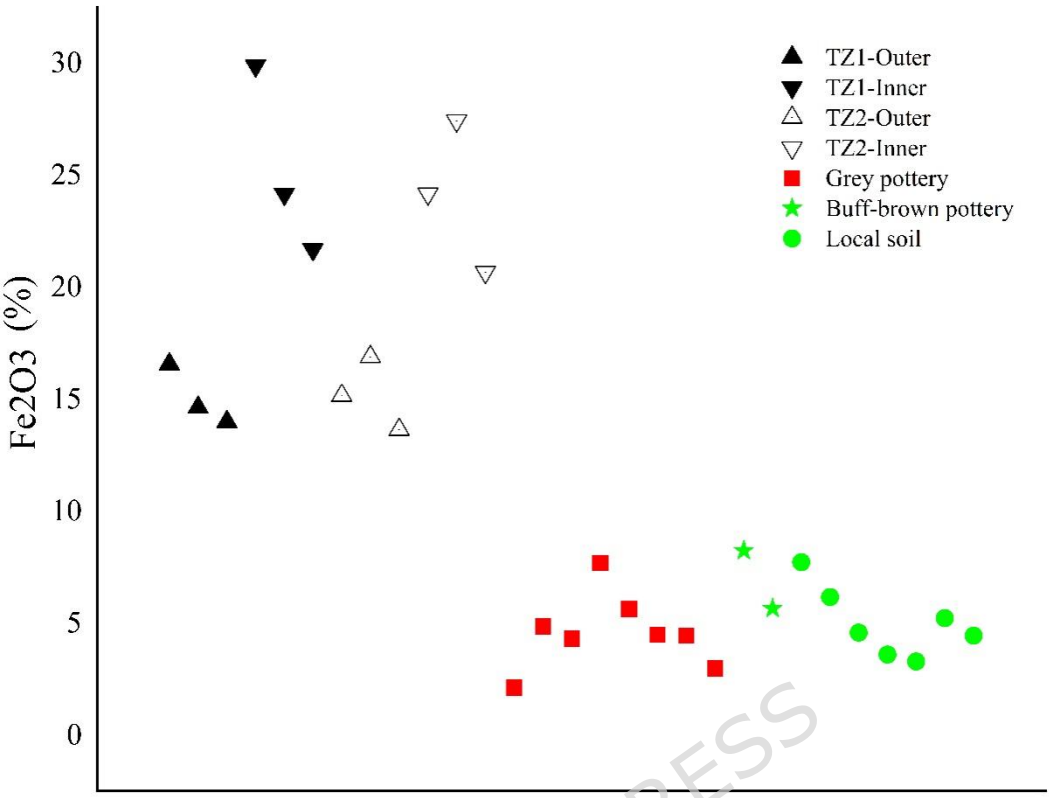


**Figure 4.** Comparison of Fe□O□ content among beads TZ1, TZ2, gray pottery and buff-brown pottery from the Nanzhuangtou site, and local soil. The beads exhibit significantly higher iron content, particularly on their inner (hollow) surfaces.



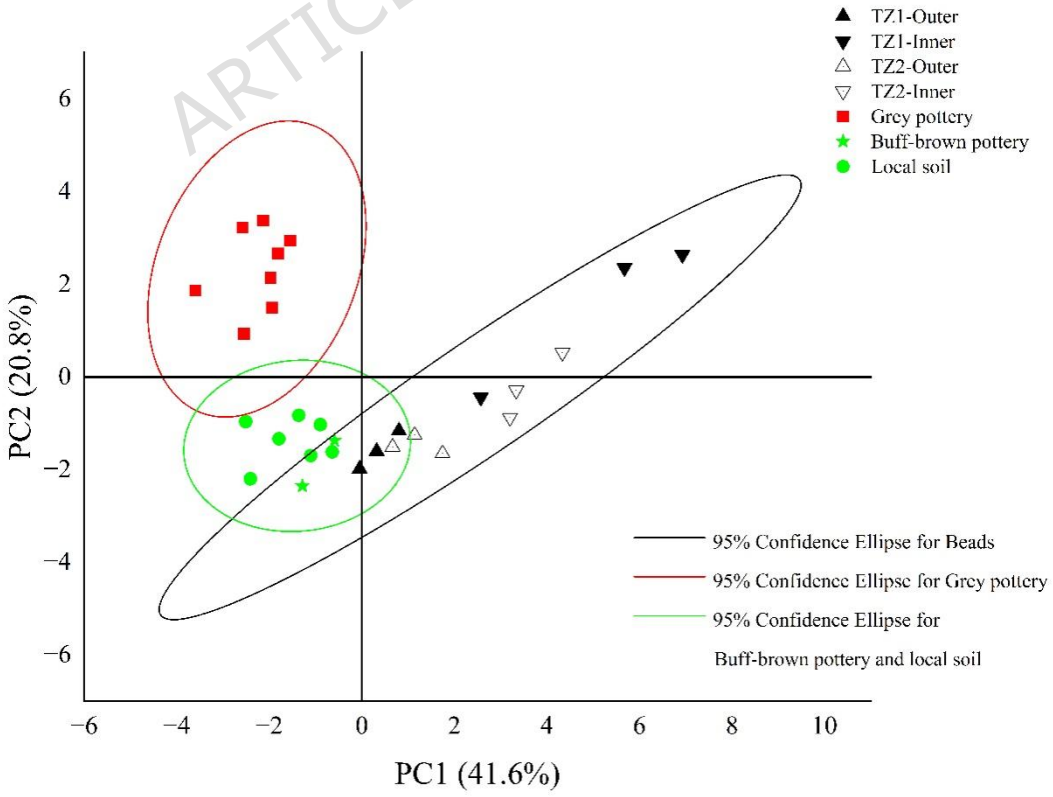

**Figure 5.** Principal component analysis based on XRF data of the ceramic beads, early pottery sherds, and local soil from the Nanzhuangtou site.

**Innovative forming technique: evidence for a plant stem mold.** A key finding of this study is the identification of the technique used to create the hollow structure. Observation via an ultradepth-of-field optical microscope revealed distinct, well-defined plant-stem-like impressions on the inner surface of TZ2 (Fig. 6). These impressions consist of dense, vertically aligned linear features with sharp boundaries, which are distributed axially. This provides direct physical evidence that a slender, rod-like organic material - most likely a plant stem or branch - was used as an inner mold around which the clay formed. This technique elegantly overcame the challenge of creating a small, thin-walled, and symmetrical tubular structure. This practice supports the hypotheses that early potters used organic materials to facilitate complex shaping during the formative stages of pottery technology[12,13]. The discovery of possible plant impressions on other early pottery from Nanzhuangtou further suggests that this was a shared technological practice within the community.

However, such clear plant impressions were not observed on the inner surface of TZ1. This discrepancy may be attributed to several factors, including variability in the intimacy of contact between the clay and the plant stem during formation, micro-erosion of the surface after firing, and the obscuring effects of burial deposits and minor abrasion over millennia. Nevertheless, the high consistency in morphology, dimensions and material composition between the two beads suggests that they belong to the same production tradition and were likely formed using the same technique - using a plant stem as an inner mold to create the hollow structure. The well-preserved impressions on TZ2 provide direct evidence of this technique, while the absence of such impressions on TZ1 reflects natural variation in the handcrafting process or differential preservation.

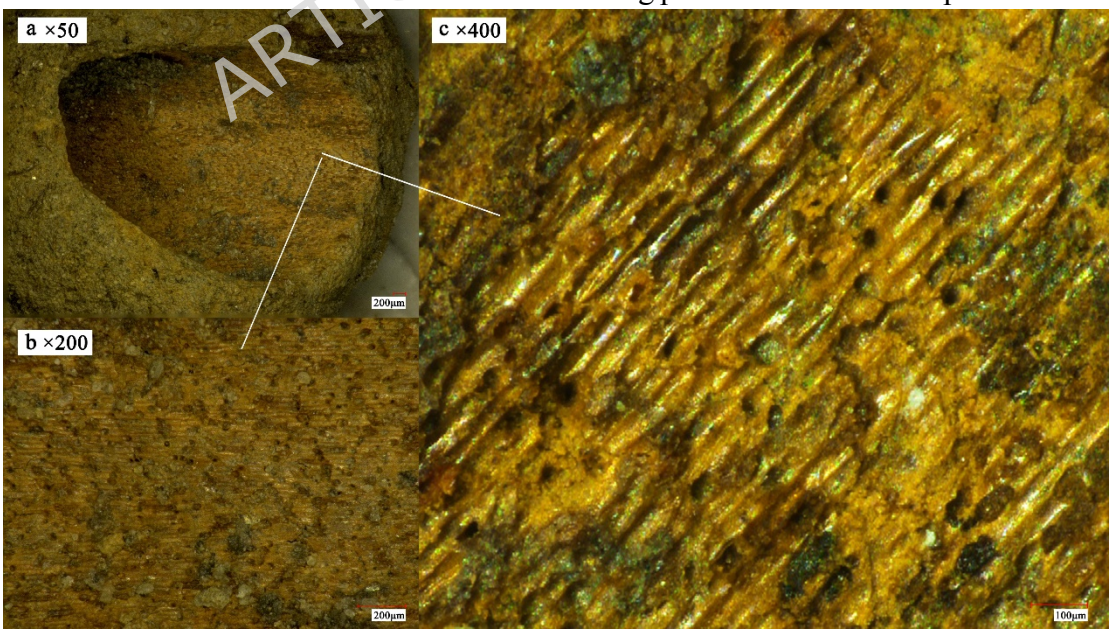


**Figure 6.** Evidence of the forming technique. Ultradepth-of-field optical micrograph of the inner surface of bead TZ2, showing distinct, vertically aligned linear impressions interpreted as evidence of a plant stem used as an inner mold during formation.

**Elementary pyrotechnology: assessment of firing conditions.** The assessment of firing technology is based on evidence from Fourier transform infrared (FTIR) analyses. Upon heating, irreversible structural changes occur in clay minerals, causing characteristic absorption peaks in their infrared spectra at 3625, 1030, 640, and 525 cm$^{-1}$ to vary with increasing firing temperature. This offers potential as a scale for discriminating between firing temperatures of ancient pottery. We performed FTIR analysis on six simulated samples with a composition similar to that of the beads [Appendix A Tab. S3]) fired at temperatures ranging from 500 to 900°. The results show a good correlation between spectral features and firing temperature (Fig. 7). The reflectance-mode FTIR spectra of the beads (Fig. 7) show that the absorption peaks for hydroxyl groups at 3625 and 2520 cm$^{-1}$ retain some intensity. This indicates that the clay minerals have not fully dehydroxylated and that the firing temperature was below 750°. The intensity of the characteristic peak for water-hydroxyl deformation vibration at 1635 cm$^{-1}$ and the two shoulder peaks at 1280 and 1100 cm$^{-1}$ is closer to that of the simulated sample fired at 500°. The faint presence of the Al-O octahedral bending vibration absorption peak at 525 cm$^{-1}$ suggests that the firing temperature was not high. Comparing the transmission-mode FTIR data (Fig. 7), the "slope" between 1030 and 1080 cm$^{-1}$ remains relatively steep. The absorbance difference (approximately 0.084) falls between the values for the samples fired at 500° (0.093) and 600° (0.065). Although the characteristic peak at 525 cm$^{-1}$ appears as a shoulder due to interference from the quartz Si-O bond absorption near 512 cm$^{-1}$, it still exhibits noticeable intensity. Based on this comprehensive analysis, the firing temperature of these two tubular ceramic artifacts is estimated to be between 500° and 600°.

This low firing temperature indicates a relatively basic level of pyrotechnological control, consistent with the characteristics reported for other early pottery from Nanzhuangtou[14]. This finding highlights the experimental and nascent nature of ceramic pyrotechnology at this early stage.



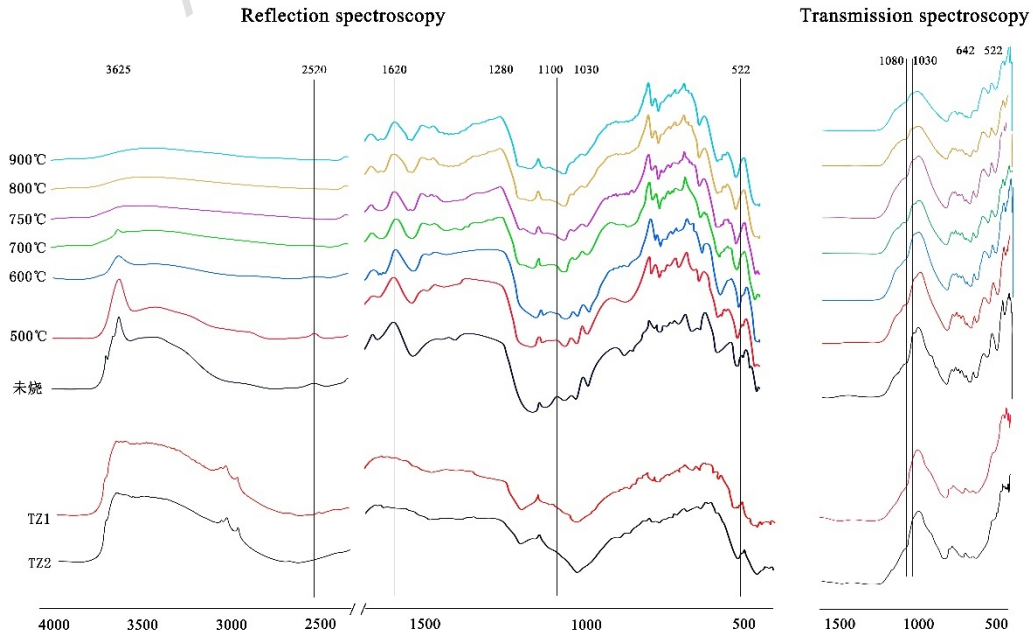

**Figure 7.** FTIR spectra of the Nanzhuangtou beads compared with experimental briquettes fired at known temperatures (500–900□), suggesting a firing range of 500–600□.

**Potential surface treatment: the use of iron oxide pigment.** The exceptionally high Fe□O□ content, as identified by X-ray fluorescence (XRF), particularly the systematic enrichment on the inner surfaces along with P□O□, requires explanation. Several non-mutually exclusive hypotheses regarding its origin have been evaluated:

1. The intentional application of an iron-oxide pigment. This hypothesis is challenged by several lines of evidence. Firstly, the enrichment is most pronounced on the inner surface, which is less accessible and visible for deliberate decoration than the outer surface. Furthermore, micro-CT imaging did not reveal a distinct, continuous layer of high-density material on the surface that would indicate an applied pigment coating (Fig. 8). The antiquity of the beads makes definitive detection of an intentionally applied, hematite-based coating difficult; long-term burial has likely caused the physical detachment or chemical alteration of any surface layer, a process exacerbated by the low firing temperature and limited sintering, which would have resulted in poor adhesion. Consistent with this, attempts to identify specific iron mineral phases (e.g. hematite) via Raman spectroscopy were inconclusive. The greater loss of material from the outer surface, which is more exposed, may also explain its lower measured iron content relative to the inner surface, which is protected.



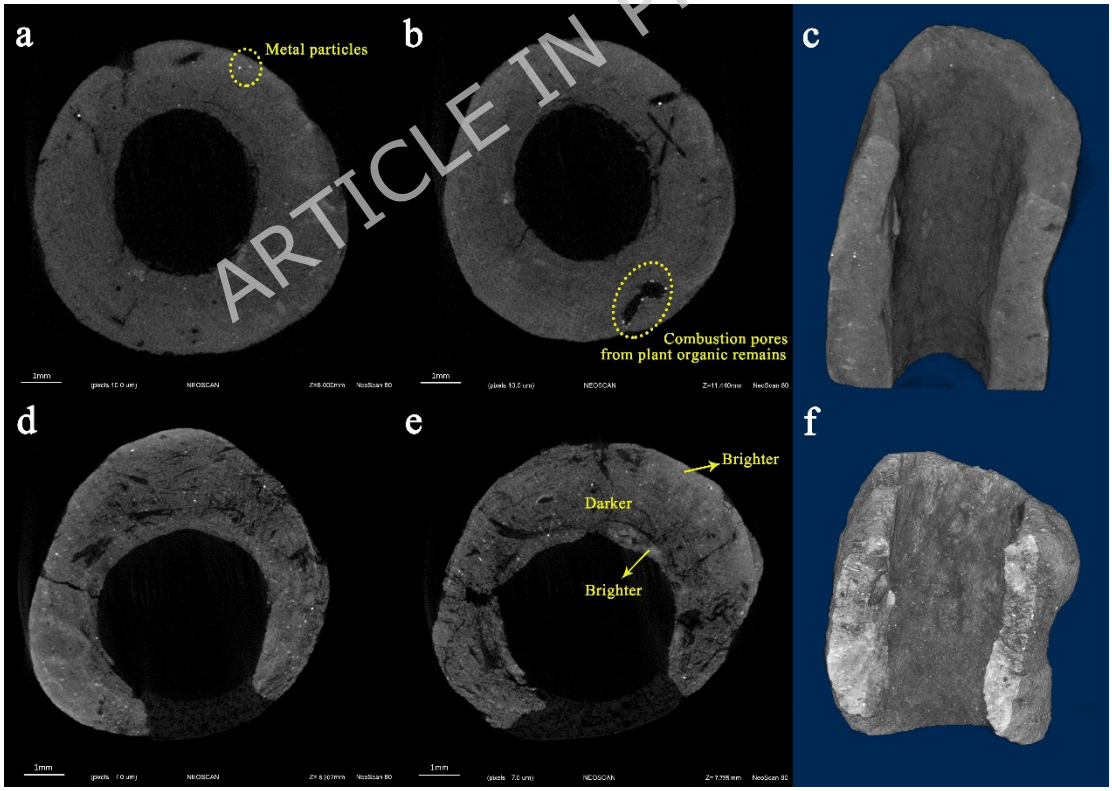


**Figure 8.** Micro-CT images of the ceramic beads. (a, b) Cross-sectional CT slice images of TZ1; (c) three-dimensional reconstruction of TZ1 based on CT slices. (d, e) Cross-sectional CT slice images of TZ2; (f) three-dimensional reconstruction of TZ2 based on CT slices.

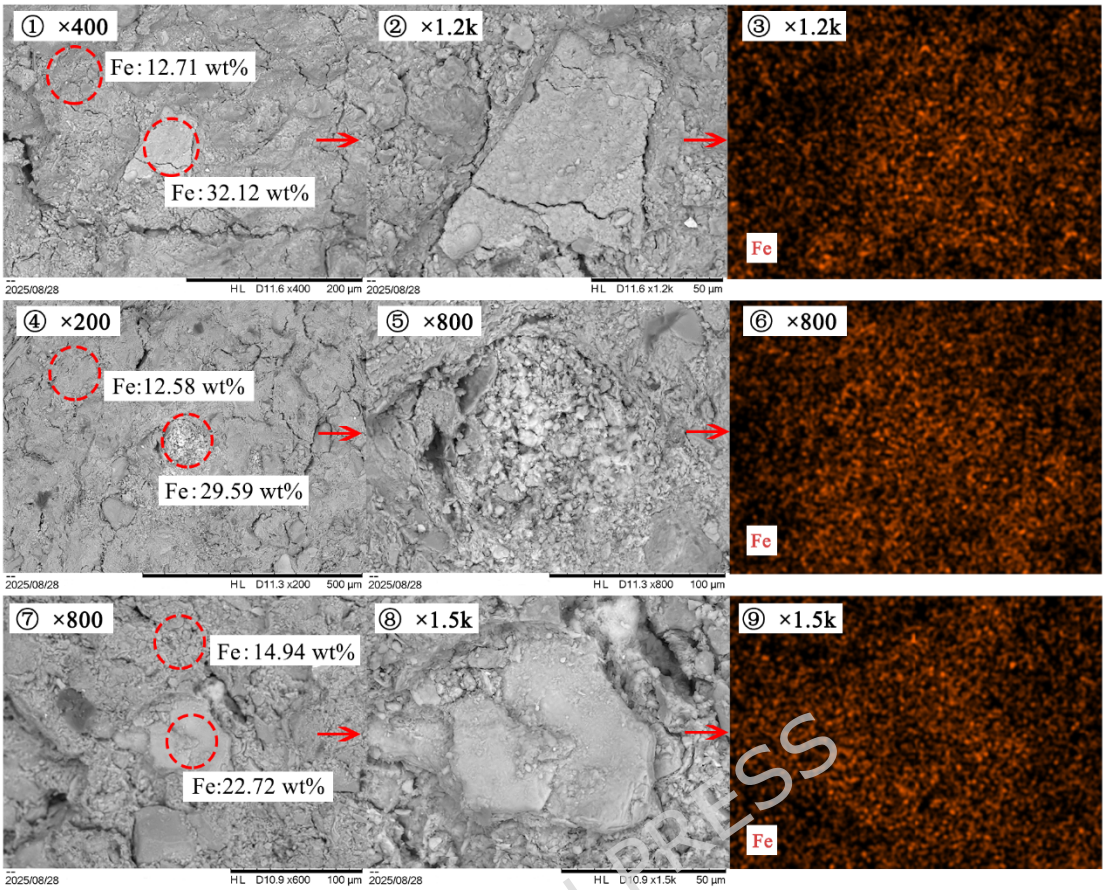


**Figure 9.** SEM images showing numerous iron-rich mineral particles on the bead surfaces, corresponding to the high Fe□O□ content detected by XRF and suggesting the possible application of a hematite-based pigment.

2. Use of naturally iron-rich clay. While the selected clay may have been iron-rich, this alone cannot explain the significant difference in composition between the inner and outer surfaces of the same bead.

3. Post-depositional diagenesis. This is considered an unlikely primary mechanism given the specificity of the enrichment to the inner wall and the co-enrichment of P□O□, which suggests a process linked to organic matter rather than general groundwater flow.

4. By-product of the plant-stem molding technique. This hypothesis aligns most coherently with the full analytical evidence and provides a unified explanation for multiple observations. Micro-CT imaging revealed several key features: (i) the inner and outer surfaces appear brighter than the interior of the ceramic body (Fig. 8e), indicating a surface concentration of metal components; (ii) numerous high-density particles (likely iron minerals) are distributed throughout the matrix (Fig. 8a); and (iii) the presence of irregular fine pores (Fig. 8b), which are judged to have been formed by the combustion of plant organic matter due to their shape, indicates that the clay mixture contained vegetal temper. Furthermore, (iv) the internal cavity is relatively straight longitudinally (Fig. 8c, f), and its morphology is consistent with the use of a rigid, rod-like inner mold. SEM confirmed the presence of numerous iron-rich particles on the outer surfaces (Fig. 9).

Crucially, these observations align with the direct evidence of plant stem impressions on the inner surface of TZ2 (Fig. 6). The plant stem used as the mold probably contained trace amounts of iron and phosphorus due to biological uptake. During low-temperature firing (500–600□), the combustion of this organic template could have facilitated the migration and secondary deposition of iron oxides onto the adjacent inner clay wall, while also enriching phosphorus. This in-situ process parsimoniously explains the co-enrichment of Fe□O□ and P□O□ on the inner surface specifically, the distribution of iron particles, and the presence of vegetal pores.

The balance of evidence thus favors Hypothesis 4, indicating that the iron enrichment was likely an unintended by-product of the manufacturing process. While possibly unrecognized by the makers, the resulting iron-rich, potentially reddish surface - especially when considered alongside the contemporary practice of applying red slips at Shangshan (9000 BP)[15] - may represent an early, incidental engagement with mineral-derived color effects in ceramic technology.

**Functional interpretation: the earliest artificial ornaments.** The interpretation of these beads as personal adornments is based on a confluence of technological, morphological, and contextual evidence, taking into account their limitations. Technologically, the use of a plant-stem mold is directly evidenced by the impressions on TZ2. While micro-CT does not provide definitive phytolithic proof, it corroborates this theory by revealing a straight, cylindrical cavity that is consistent with a rigid stem. Morphologically, the hollow, tubular, thin-walled form is an archetypal design for stringing. The slight asymmetry in profile is a feature commonly seen in pendants across cultures and serves to stabilize the object's orientation when suspended. A systematic use-wear analysis was conducted on the surfaces of both beads using a KEYENCE VHX-2000 ultra-depth 3D microscope at magnifications ranging from ×50 to ×400, with the aim of identifying characteristic micro-polish or linear striations indicative of suspension. However, due to extensive post-depositional surface alteration—including micro-pitting, abrasion, and mineral accretion—the analysis was inconclusive, and no definitive microwear traces could be discerned. Nevertheless, the morphology itself strongly suggests that the object was intended to be hung. Furthermore, the small size and fragile, thin-walled construction argue against a practical, utilitarian function, such as that of components of tools or weapons.

Several possibilities for alternative functions can be reasonably discounted. They are unlikely to be spindle whorls due to their minimal mass and asymmetric form. There is also no evidence to suggest that they were used as applicators, measuring devices or ritual objects distinct from adornment. Given the absence of utilitarian traits, the most parsimonious explanation is that they were crafted for display. Most significantly, the considerable technical investment in crafting such small, non-utilitarian items suggests a symbolic or aesthetic purpose, translating the enduring human tradition of ornamentation into a new medium created by humans.

When viewed alongside the long□standing human tradition of wearing perforated natural materials for decoration, these ceramic beads represent an early technological

translation of that tradition into a new, entirely synthetic medium. This aligns with the definition of 'artificial materials' in this study, which are substances created by actively intervening in natural processes to induce irreversible chemical and physical transformations, rather than merely modifying natural forms. As the earliest such material, pottery perfectly embodies this concept: shaping clay and firing it at high temperatures induces irreversible dehydration and vitrification of silicate minerals, yielding a new, hard, and water□resistant inorganic non□metallic material. The form, manufacturing technique, and archaeological context of the beads all support the interpretation that they are personal ornaments. They represent an innovative stage in the use of fully synthetic ceramic materials for symbolic expression, and are currently the earliest known example. The world's oldest widely recognized ornaments made from artificial materials are glazed steatite beads from Period III at Mehrgarh in South Asia[16] and from the Badarian civilization in Predynastic Egypt[17], dating to around the 4th millennium BCE. These steatite beads were glazed and fired to produce a glossy surface layer, and evidence suggests the use of copper-based colorants. The earliest ceramic beads found outside China were terracotta beads from the Ravi phase at Harappa in the Indus Valley[18], dating to 3700–2800 BCE (Period 1A/1B, Ravi phase). These beads exhibit diverse shapes, often formed by hand modelling or rolling, with perforations made using reed stems or porcupine quills, and fired using simple techniques, likely in open fires or during pottery firing. In China, the earliest known ceramic bead ornaments are a pottery pendant from phase III at Jiangzhai[19]. It is made of fine red clay, is olive-shaped, and has a central perforation.

A comparative overview of these key contexts is presented in Tab. 2. Compared with the earliest ornaments made from artificial materials found in regions such as South Asia and Egypt, the Nanzhuangtou beads date from an earlier period, the Palaeolithic-Neolithic transition. Technologically, the Nanzhuangtou beads are characterized by their high Fe□O□ content. Clear impressions of plant stems on the inner walls confirm that a plant "inner mold" was used to form their hollow structure. The low firing temperature of 500–600□ indicates basic firing technology. Surface wear patterns suggest that the beads were strung and worn as personal adornments. Their morphology and technological attributes are consistent with the technological level of the early to middle Neolithic period in North China.

**Table 2.** Comparative overview of the earliest known artificial ornaments from key archaeological contexts

| Site / Region | Approximate Date (BCE/BP) | Material | Key Manufacturing Techniques | Morphology & Remarks |
|---|---|---|---|---|
| Nanzhuangtou, China | 10,000 cal BP | Ceramic (clay) | Local clay; plant-stem inner mold; low-temperature firing (500–600□) | Hollow tubular beads; asymmetric profile; possible surface treatment with iron-rich pigment |
| Mehrgarh, South Asia | 4000 BCE (Period III) | Glazed steatite | Steatite shaping; glazing with copper-based colorants; high-temperature firing | Various shapes (discs, cylinders); glossy surface; often blue-green glaze |

| | | | | |
|---|---|---|---|---|
| Harappa, Indus Valley | 3700–2800 BCE (Ravi Phase) | Terracotta (clay) | Hand-modelling or rolling; perforation with reed stems or quills; open-fire/low-temperature firing | Diverse shapes (barrel, bicone, cylinder); often undecorated or simply impressed |
| Jiangzhai, China | 4000–3000 BCE (Phase III) | Ceramic (fine red clay) | Hand-forming; central perforation; firing | Olive-shaped pendant with central perforation |

Based on the analytical results, the two tubular ceramic beads unearthed from gully G1 at the Nanzhuangtou site may be the earliest known ornaments made from artificial materials. This discovery not only sheds light on the aesthetic practices and technical ingenuity of ancient peoples from around 10,000 years ago, but also provides crucial empirical evidence for exploring the evolution of prehistoric ornamentation and the origins of the use of artificial materials.

## Conclusions

Integrated analyses, including high-resolution micro-CT, XRF, SEM, and FTIR, provide strong evidence that the two tubular ceramic beads from Nanzhuangtou are among the earliest known ornaments manufactured from a synthetic material. Their chronological placement at approximately 10,000 cal BP is securely established through stratigraphic association with directly dated organic materials from the sealed context of Gully G1 and the overlying layer ③. While direct radiocarbon dating of the beads themselves was not undertaken due to their exceptional rarity and fragility, the consistent and coherent chronological framework provided by the associated samples robustly anchors them to the Palaeolithic-Neolithic transition in North China.

The data indicate a production process involving the use of local clay, shaping around a plant-stem mold and low-temperature firing (500–600□). The pronounced iron enrichment on the inner surfaces is most parsimoniously interpreted as an unintended by-product of this organic molding technique. Their morphology and context are consistent with their use as personal adornments. This discovery provides compelling evidence that early ceramic technology was used for symbolic expression during the Palaeolithic-Neolithic transition, offering new insights into the early use of synthetic materials for personal adornment.

## Methods

**Radiocarbon dating.** The chronological context of the ceramic beads is defined by the radiocarbon dating of organic material that is securely associated with the beads within the same sealed context (Gully G1). Due to the exceptional rarity and fragility of these artifacts, direct dating of the beads themselves was not undertaken. To establish a robust age, a wood sample from gully G1 was directly dated. For broader chronological reference, the date from the basal part of the overlying layer ③, as reported in the original excavation report[10], is also presented. All samples were analysed at the Peking University AMS $^{14}$C Laboratory. The conventional radiocarbon ages were calibrated via the IntCal20 atmospheric curve (Reimer et al. 2020) and the OxCal v4.4.4 program

(Bronk Ramsey, 2021). The calibrated results from both contexts are stratigraphically coherent and closely aligned in time. This provides a consistent chronological framework that securely dates the beads to approximately 10,000 years BP, placing them in the initial phase of the Palaeolithic-Neolithic transition in North China.

**Chemical composition analysis.** The chemical composition of the beads was determined via a HORIBA XGT-9000 X-ray fluorescence (XRF) spectrometer. Calibration was performed using standard reference materials before testing. The inner and outer surfaces of each bead were analysed. The X-ray beam was generated at 50 kV and 316 μA, with a live time of 100 s per measurement. A grid analysis was performed in spectrum mode, covering a 1 mm × 1 mm square area with a 0.2 mm step interval, resulting in 25 measurement points per grid. The elemental ratios for the oxides were calculated using the fundamental parameters method, and all results are presented as weight percentages (wt%). The measured data for each sample include 17 oxides: MgO, $Al_2O_3$, $SiO_2$, $P_2O_5$, $SO_3$, $K_2O$, CaO, $TiO_2$, $V_2O_5$, $MnO_2$, $Fe_2O_3$, ZnO, $Rb_2O$, SrO, $ZrO_2$, PdO, and $SnO_2$, with the principal clay elements, such as Si, Al, Fe, Ca, Mg, and K being of primary interest.

**Non-destructive microscopic observation of sample surfaces**. A KEYENCE VHX-2000 ultra-depth 3D microscope system (for images Fig. 6) and a NIKON ShuttlePix P-MFSC Microscope were used for non-destructive microscopic observation of the samples. All photographs were taken using the vivid and clear 3D stereoscopic observation function.

**Microstructural observation and localized elemental analysis**. Microstructural observation and localized elemental analysis were conducted via a HITACHI TM4000 tabletop scanning electron microscope (SEM) equipped with a BRUKER energy-dispersive X-ray spectroscopy (EDS) system. No sample preparation was performed on the ceramic beads, which were placed directly on a sample stage with conductive tape to acquire SEM images and EDS data from the relatively flat surfaces of the beads. The analysis was performed at an accelerating voltage of 15 kV.

**Firing temperature estimation**. To obtain ideal results for estimating the firing temperature of the ceramic products, this study involved designing a set of simulated pottery firing experiments with gradient temperature increases. Soil from near the Xushui area in Hebei (primarily composed of kaolin and iron ore rock soil) was selected to create the simulated samples. Analysis of the soil's chemical composition showed that the major component contents, such as SiO□, Al□O□, and Fe□O□, in the simulated clay were relatively consistent with those of the beads (Appendix A, Tab. S3). A certain amount of water was added to the clay and mixed thoroughly to form lumps. Fourteen simulated samples measuring approximately 8×6×1 cm (length×width×height) were then hand-formed from these lumps and air-dried at room temperature for 36 hours. A muffle furnace equipped with an intelligent REX-C700 temperature controller was used to heat the simulated samples. Starting from 500□, two

samples were fired at 100□ intervals up to a maximum temperature of 800□ (including 750□). The samples were held at each temperature for 4 hours and cooled to room temperature after firing.

To minimize potential damage to the archaeological specimens during measurement, a PIKE diffuse reflection accessory was initially used for non-destructive infrared analysis in reflectance mode. However, obvious interference peaks from organic contaminants were observed in the results obtained from the non-destructive mode, so a Thermo Scientific Nicolet Summit FTIR spectrometer was used for micro-destructive infrared testing in transmission mode. Testing was performed by scraping off only a small quantity of powder, without standardized sample preparation.

Spectra were collected over a range of 4000 to 400 $cm^{-1}$, with 32 scans per measurement and a spectral resolution of 4 $cm^{-1}$. Data acquisition was performed via Thermo Scientific OMNIC Paradigm software. The resulting spectra were subsequently processed with EZ OMNIC software for automatic baseline correction and smoothing. Final data compilation and plotting were conducted via Origin 2024 software.

**Micro-CT observation**. CT analysis was conducted using a high-resolution Neoscan N80 desktop micro-CT system. The samples (TZ1 and TZ2) were mounted on a sample holder and scanned. The following scanning parameters were used: voltage 84 kV, current 48 μA. The pixel sizes were 10 μm and 7 μm for TZ1 and TZ2, respectively. After scanning, the acquired data were reconstructed and processed using the accompanying software to obtain cross-sectional views and three-dimensional images.

**Ethics statement**. Permission was obtained from the Hebei Provincial Institute of Cultural Relics and Archaeology for the collection and analysis of the ceramic beads used in this study.



## Data availability

All the analytical data gathered during the study are fully reported in this paper.

## References


1. Ma, Q. Study on personal ornaments in Chinese Palaeolithic. *Master Thesis, Hebei Normal University* (In Chinese) (2016).
2. Wei, Y., D'Errico, F. & Gao, X. Research status and significance of Palaeolithic ornaments. *Acta Anthropologica Sinica* **35**(1), 1–15 (In Chinese) (2016).
3. Zabiako, A.П. & Wang, J.Z. Palaeolithic ornaments from Xiaogushan, Haicheng and Eurasian prehistoric symbolism. *Inner Mongolia Cultural Relic and Archaeology* (2), 1–9 (In Chinese) (2024).
4. Huang, W.W. *et al*. Bone artifacts and ornaments from Xiaogushan, Haicheng. *Acta Anthropologica Sinica* **5**(3), 231–240 (In Chinese) (1986).
5. Wang, C.X. *et al*. Study on ostrich eggshell ornaments from Shuidonggou site. *Chinese Science Bulletin* **54**(19), 3521–3527 (In Chinese) (2009).
6. Li, C.R. The ornament-loving Upper Cave people of Beijing. *Fossils* (4), 28–31 (In Chinese) (2019).

7. Ke, W.W. Technological analysis of Palaeolithic ornaments unearthed in China. *Comparative Study of Cultural Innovation* **4**(34), 156–158 (In Chinese) (2020).
8. Cui, J. *Research on prehistoric jewelry in China* Master Thesis, Xi'an University of Science and Technology (In Chinese) (2024).
9. Ayrton, E.R. & Loar, W.L.S. *Predynastic Cemetery at El Mahasna*. (Egypt Exploration Fund ,1911).
10. Xu, H.S., Jin, J.G. & Yang, Y.H. Preliminary report of Nanzhuangtou site in Xushui, Hebei. *Archaeology* (11), 961–970 (In Chinese) (1992).
11. Li, J., Qiao, Q. & Ren, X.Y. Excavation report of Nanzhuangtou site in Xushui, Hebei in 1997. *Acta Anthropologica Sinica* (3), 321–350 (In Chinese) (2010).
12. Yuan, J.R. Rice and pottery before 10,000 years ago from Yuchanyan, Daoxian, Hunan. In *Origins of Rice Cultivation, Pottery and Cities* (eds Yan, W.M. & Yasuda, Y.), 45-52 (In Chinese) (Cultural Relics Press, 2000).
13. Liu, S. Cui, J.F. & Wang LX. Scientific analysis of pottery sherds from Houtaomuga site, Da'an, Jilin. *Research of China's Frontier Archaeology* (1), 34–45 (In Chinese) (2017).
14. Ren, X.Y. *et al*. Study on firing temperature of early pottery from Nanzhuangtou site. *Rock and Mineral Analysis* **29**(2), 156–160 (In Chinese) (2010).
15. Jiang, L.P. Preliminary report on the excavation of the Shangshan site in Pujiang County, Zhejiang. *Archaeology* (9), 7–18 (In Chinese) (2007).
16. Bouquillon, A. *et al*. Glazed steatite beads from Mehrgarh and Nausharo (Pakistani Balochistan). *MRS Online Proceedings Library* **352**, 527–538 (1995).
17. Alwardany, R.A. Glazed steatite in Ancient Egypt. *International Journal of Advanced Studies in World Archaeology*, 43–63 (2023).
18. Kenoyer, J. M. Bead technologies at Harappa, 3300–1900 BC: a comparative summary. In *South Asian Archaeology* (eds Jarrige, C. & Lefèvre, V.), 157–170 (Éditions Recherche sur les Civilizations, 2001).
19. Banpo, Museum. *Jiangzhai: Excavation Report of a Neolithic Site*, 274 (In Chinese) (Cultural Relics Press, 1988).
20. Liu, S.R., Gong, X. & Yan, B.C. Infrared spectral analysis of firing temperature of ancient pottery. *Spectroscopy and Spectral Analysis* **43**(5), 1350–1355 (In Chinese) (2023).

## Author contributions

Jianxiang Chen and Jingfang Zhao are co-first authors who contributed equally to this work. They designed the research and wrote the paper. Jianxiang Chen performed the experiments. Jingfang Zhao is the corresponding author. Jun Li, Wenrui Zhang and Xueyan Ren provided samples. Kai Wang provided guidance on the experimental design. Wanli Zhao and Wen Gao contributed to the discovery of the samples.

## Funding

This work is supported by the special project "Study on the Transition Pattern of the Palaeolithic–Neolithic Period in Northern North China" under the "Study on Major Historical Issues" of the Chinese Academy of History, The National Social Science Fund of China (23VLS005).

## Competing interests

The authors declare that they have no competing interests.

# Appendix A. Supplementary material

**Table S1** Chemical composition (representative points, wt%) of the ceramic beads from the Nanzhuangtou site

| Sample ID | MgO | $Al_2O_3$ | $SiO_2$ | $P_2O_5$ | $SO_3$ | $K_2O$ | CaO | $TiO_2$ | $V_2O_5$ | $MnO_2$ | $Fe_2O_3$ | ZnO | $Rb_2O$ | SrO | $ZrO_2$ | PdO | $SnO_2$ |
|---|---|---|---|---|---|---|---|---|---|---|---|---|---|---|---|---|---|
| TZ1 Outer-1 | 2.07 | 12.74 | 59.40 | 0.29 | 0.25 | 3.02 | 4.35 | 0.75 | 0.10 | 0.06 | 16.56 | 0.02 | 0.02 | 0.02 | 0.01 | 0.06 | 0.26 |
| TZ1 Outer-2 | 2.46 | 15.01 | 60.80 | 0.38 | 0.14 | 2.91 | 2.49 | 0.67 | 0.09 | 0.07 | 14.62 | 0.02 | 0.02 | 0.02 | 0.01 | 0.06 | 0.23 |
| TZ1 Outer-3 | 2.55 | 14.38 | 62.74 | 0.29 | 0.06 | 2.87 | 1.99 | 0.67 | 0.07 | 0.03 | 13.99 | 0.02 | 0.02 | 0.02 | 0.02 | 0.06 | 0.22 |
| TZ1 Inner-1 | 1.98 | 11.18 | 44.21 | 1.97 | 0.67 | 2.13 | 5.62 | 0.58 | 0.37 | 0.73 | 29.88 | 0.02 | 0.04 | 0.03 | 0.02 | 0.10 | 0.47 |
| TZ1 Inner-2 | 2.18 | 14.13 | 48.33 | 1.01 | 1.06 | 2.53 | 4.33 | 0.80 | 0.29 | 0.66 | 24.15 | 0.02 | 0.03 | 0.03 | 0.02 | 0.10 | 0.34 |
| TZ1 Inner-3 | 1.92 | 12.94 | 54.25 | 0.89 | 0.13 | 2.76 | 4.13 | 0.56 | 0.15 | 0.03 | 21.68 | 0.08 | 0.03 | 0.03 | 0.02 | 0.09 | 0.31 |
| TZ2 Outer-1 | 2.14 | 12.61 | 62.00 | 0.77 | 0.19 | 2.67 | 2.97 | 0.68 | 0.11 | 0.04 | 15.16 | 0.09 | 0.02 | 0.03 | 0.11 | 0.08 | 0.34 |
| TZ2 Outer-2 | 2.29 | 13.68 | 59.72 | 0.38 | 0.15 | 2.99 | 2.58 | 0.71 | 0.09 | 0.05 | 16.89 | 0.02 | 0.02 | 0.02 | 0.03 | 0.07 | 0.31 |
| TZ2 Outer-3 | 2.25 | 13.20 | 63.15 | 0.51 | 0.19 | 3.10 | 2.73 | 0.65 | 0.08 | 0.06 | 13.64 | 0.02 | 0.02 | 0.03 | 0.05 | 0.07 | 0.25 |
| TZ2 Inner-1 | 1.75 | 9.92 | 55.47 | 1.03 | 0.28 | 2.78 | 3.21 | 0.50 | 0.21 | 0.08 | 24.17 | 0.02 | 0.03 | 0.03 | 0.02 | 0.09 | 0.41 |
| TZ2 Inner-2 | 1.82 | 9.58 | 52.41 | 1.23 | 0.44 | 2.04 | 3.52 | 0.54 | 0.24 | 0.15 | 27.43 | 0.02 | 0.04 | 0.03 | 0.02 | 0.09 | 0.42 |
| TZ2 Inner-3 | 2.04 | 11.56 | 56.98 | 0.86 | 0.25 | 2.67 | 3.43 | 0.58 | 0.19 | 0.11 | 20.67 | 0.02 | 0.03 | 0.03 | 0.10 | 0.09 | 0.40 |

**Table S2** Chemical composition (mean values, wt%) of the early buff-brown pottery from the Nanzhuangtou site

| Sample ID | MgO | $Al_2O_3$ | $SiO_2$ | $P_2O_5$ | $SO_3$ | $K_2O$ | CaO | $TiO_2$ | $V_2O_5$ | $MnO_2$ | $Fe_2O_3$ | ZnO | $Rb_2O$ | SrO | $ZrO_2$ | PdO | $SnO_2$ |
|---|---|---|---|---|---|---|---|---|---|---|---|---|---|---|---|---|---|
| G3:89 | 2.32 | 17.13 | 63.82 | 0.29 | 0.13 | 3.51 | 3.21 | 0.91 | 0.07 | 0.04 | 8.23 | 0.02 | 0.02 | 0.02 | 0.02 | 0.07 | 0.20 |
| Standard Deviation | 0.06 | 0.79 | 1.23 | 0.03 | 0.03 | 0.15 | 0.19 | 0.09 | 0.01 | 0.01 | 0.51 | 0.00 | 0.00 | 0.00 | 0.00 | 0.00 | 0.02 |
| T4⑤:1 | 2.08 | 15.05 | 68.03 | 0.32 | 0.05 | 3.67 | 4.47 | 0.80 | 0.06 | 0.05 | 5.04 | 0.02 | 0.02 | 0.03 | 0.07 | 0.07 | 0.17 |
| Standard Deviation | 0.50 | 2.46 | 2.83 | 0.21 | 0.11 | 0.82 | 2.22 | 0.09 | 0.00 | 0.02 | 1.56 | 0.00 | 0.00 | 0.01 | 0.08 | 0.01 | 0.03 |

**Table S3** Comparison of chemical composition (mean values, wt%) between Nanzhuangtou ceramic beads and simulated pottery-firing samples

| Sample ID | $SiO_2$ | $Al_2O_3$ | $Fe_2O_3$ | CaO | MgO | $K_2O$ | $Na_2O$ |
|---|---|---|---|---|---|---|---|
| TZ1 Outer | 56.57 | 14.00 | 20.28 | 3.44 | 2.69 | 2.96 | 0.07 |
| TZ1 Inner | 61.46 | 13.91 | 16.25 | 2.78 | 2.59 | 2.69 | 0.33 |
| TZ2 Outer | 60.17 | 13.57 | 15.95 | 4.83 | 2.15 | 2.80 | 0.54 |
| TZ2 Inner | 62.54 | 12.55 | 16.16 | 3.19 | 2.19 | 2.76 | 0.61 |
| Simulated-1 | 66.58 | 12.37 | 13.17 | 1.84 | 0.87 | 2.49 | 2.69 |
| Simulated-2 | 63.94 | 12.73 | 14.58 | 2.70 | 0.94 | 2.39 | 2.72 |
| Simulated-3 | 64.00 | 12.62 | 14.33 | 3.08 | 0.82 | 2.53 | 2.63 |
| Simulated-4 | 66.27 | 11.65 | 13.47 | 2.92 | 0.87 | 2.26 | 2.55 |